frontiers | Frontiers in Marine Science

TYPE Original Research
PUBLISHED 11 July 2024
DOI 10.3389/fmars.2024.1412052



OPEN ACCESS

EDITED BY
Chengji Shen,
Hohai University, China

REVIEWED BY
Yunhai Fang,
Hefei University of Technology, China
Zhang Bo,
Shandong University of Science and Technology, China
Qiguo Sun,
Jiangsu University of Science and Technology, China
Zenhom Salem,
Tanta University, Egypt
Venkatramanan Senapathi,
National College, Tiruchirappalli, India

*CORRESPONDENCE
Xilai Zheng
zhxilai@ouc.edu.cn

RECEIVED 04 April 2024
ACCEPTED 27 June 2024
PUBLISHED 11 July 2024

CITATION
Chang Q, Gao C, Zheng X, Lin Y and Song X (2024) A novel subsurface adjustable dam for preventing active seawater intrusion in coastal aquifers.
*Front. Mar. Sci.* 11:1412052.
doi: 10.3389/fmars.2024.1412052



# A novel subsurface adjustable dam for preventing active seawater intrusion in coastal aquifers

Qinpeng Chang[1,2], Chenchen Gao[1,3], Xilai Zheng[1,3]*, Yucheng Lin[1,3] and Xiaoran Song[4]

[1]College of Environmental Science and Engineering, Ocean University of China, Qingdao, China, [2]College of Marine Geosciences, Ocean University of China, Qingdao, China, [3]Key Laboratory of Marine Environment and Ecological Education, Ministry of Education, Ocean University of China, Qingdao, China, [4]Personnel Office, Qingdao Hydrological Center, Qingdao, Shandong, China

Subsurface physical barriers are widely used to prevent seawater intrusion in the world. After the construction of physical barriers, the residual saltwater is trapped upstream the barriers. Traditional physical barriers, including cutoff walls and subsurface dams, are fixed in structure and fail in prohibiting active seawater intrusion. In this work, a novel subsurface adjustable dam, composed of dam bodies and sluice gates, was designed to prevent active seawater intrusion and store groundwater flexibly according to seasonal variations in precipitation. We set three-dimensional field-scale numerical simulations to compare the control effects of adjustable dams, cutoff walls, and subsurface dams. The results revealed that the traditional subsurface physical barriers could mitigate the velocity of active seawater intrusion but were inadequate in completely preventing the intrusion process. Furthermore, although the traditional physical barriers temporarily alleviate the residual saltwater during the wet periods, the saltwater wedge would subsequently invade during next dry periods. Thus, the salt mass in the aquifer of traditional physical barriers scenarios exhibited a gradual annual increase. In contrast, the novel subsurface adjustable dam demonstrated the ability to prevent active seawater intrusion and remove the residual saltwater. During the dry periods, characterized by low precipitation recharge, the sluice gates were closed to obstruct the path of active seawater intrusion. Conversely, during the wet periods with abundant precipitation, the sluice gates were opened, facilitating the gradual removal of the residual saltwater. The flexible adjustment mechanism of subsurface adjustable dams resulted in a annual decrease in both the seawater intrusion length and the salt mass in the entire aquifer. These findings underscore the efficacy of the subsurface adjustable dam as a measure for preventing active seawater intrusion and simultaneously eliminating the residual saltwater.

KEYWORDS

**active seawater intrusion, coastal aquifer, cutoff wall, subsurface dam, adjustable dam**

# 1 Introduction

The exacerbating impacts of excessive groundwater extraction and rising sea levels have intensified seawater intrusion (SWI) in coastal aquifers, posing significant threats to groundwater quality (Lu et al., 2013; LeRoux et al., 2023). The implementation of subsurface physical barriers has emerged as an effective countermeasure to mitigate SWI and safeguard groundwater resources (Kong et al., 2023). Furthermore, the subsurface physical barriers can serve as groundwater reservoirs which augments fresh groundwater storage (Ishida et al., 2011). Thus, subsurface physical barriers have gained widespread adoption in coastal regions globally, including China, Japan, India, the Middle East, and South America (Zheng et al., 2020; Chang et al., 2023).

Traditional subsurface physical barriers fall into three primary categories: cutoff walls, subsurface dams, and full-section physical barriers (Kaleris and Ziogas, 2013). Subsurface dams impede the lower portion of the aquifer while maintaining an upper opening for discharge. Conversely, cutoff walls are constructed in the upper portion of the aquifer, leaving a lower opening for discharge. Luyun et al. (2011) demonstrated that the efficacy of cutoff walls in preventing SWI was comparable to that of recharge wells. Chang et al. (Chang et al., 2019, 2020) introduced the concept of minimum effective height for subsurface dams in SWI prevention, and attributed the upward movement of the saltwater wedge to the obstruction caused by subsurface dams. Subsequently, Chang et al. (Chang et al., 2021, 2022) investigated the mechanism of cutoff walls in SWI prevention and proposed optimization strategies. Shen et al. (2020) analyzed the impact of tidal forces and cutoff walls on groundwater flow and salinity distribution in coastal aquifers, revealing that tidal influence enhances the effectiveness of cutoff walls in SWI mitigation. Zheng et al. (Zheng et al., 2021, 2022) examined the dynamic desalination process of the residual saltwater trapped upstream the subsurface dams and cutoff walls. They suggested that the desalination time for subsurface dams can be protracted for decades, while that for cutoff walls is typically several years. Furthermore, Yin et al. (2023) proposed combining saltwater discharge or freshwater recharge to expedite the desalination of the residual saltwater upstream subsurface dams. On the other hand, field investigations of groundwater quality have indicated that the implementation of subsurface physical barriers can lead to the accumulation of land-based pollutants (Kang and Xu, 2017). Fang et al. (2021) and Sun et al. (2019) employed indoor experiments and numerical simulations to elucidate the mechanism of nitrate accumulation induced by cutoff walls and subsurface dams. Recently, a novel mixed physical barrier, integrating a cutoff wall and a subsurface dam, has been developed to enhance SWI prevention and facilitate the removal of the residual saltwater (Abdoulhalik and Ahmed, 2017; Gao et al., 2021).

Previous research on subsurface physical barriers has predominantly focused on passive seawater intrusion (SWI), where the inland groundwater level exceeds the seawater level (Gao et al., 2022; Wang et al., 2023). However, in numerous coastal regions experiencing excessive groundwater extraction, the inland groundwater level falls below sea level during the dry periods, leading to active SWI (Badaruddin et al., 2017). Unfortunately, none of the existing subsurface physical barriers, including cutoff walls, subsurface dams, or mixed barriers, can effectively prevent active SWI due to their bottom or top apertures for groundwater discharge. Thus, previous studies on traditional physical barriers have been limited to passive SWI. The impermeable full-section physical barrier, which completely obstructs the seepage path, has the potential to prevent active SWI. However, it may result in the accumulation of land-based contaminants in inland aquifers (Ishida et al., 2011; Kang and Xu, 2017). Moreover, the residual saltwater upstream of subsurface dams can persist for decades due to the obstruction, raising concerns about chronic saltwater contamination (Zheng et al., 2021; Chang et al., 2024). As a result, the impermeable full-section physical barrier has been gradually abandoned by researchers and designers.

Unlike the subsurface dam and cutoff wall, the subsurface permeable reactive barrier employs vertical openings to facilitate the flow of contaminant plumes through the reactive media (Figure 1A) (Blowes et al., 2000). Similarly, gated storm surge barriers, designed to mitigate coastal flood hazards during extreme storms, incorporate vertical auxiliary lift gates that are only closed during coastal flooding events (Figure 1B) (Orton et al., 2023). Inspired by the designs of subsurface permeable reactive barriers and gated storm surge barriers, we propose a novel subsurface adjustable dam consisting of high underground dam bodies and adjustable vertical sluice gates (Figure 2). The sluice

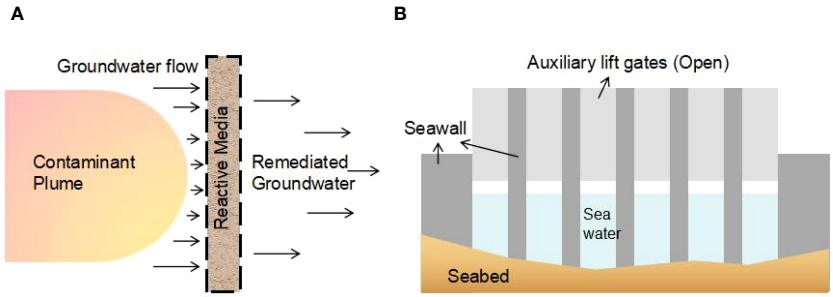


FIGURE 1
Schematics of **(A)** the overhead view of the subsurface permeable reactive barrier and **(B)** the elevation view of the storm surge barrier which includes auxiliary lift gates.

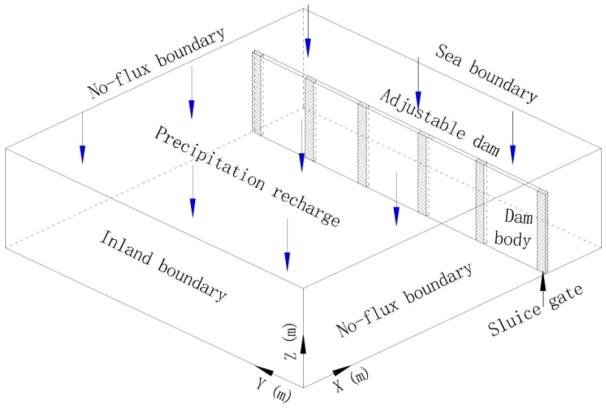


FIGURE 2
Schematic diagram of the conceptual model.

gates are integrated within the dam bodies, mimicking the structure of storm surge barriers with auxiliary lift gates (Figure 1B). Groundwater discharge is controlled by the sluice openings, which can be opened or closed in response to dynamic variations in precipitation. During the dry periods, the sluice gates are closed to conserve groundwater resources and prevent active SWI. Conversely, during the wet periods, the sluice gates can be opened to discharge the residual saltwater upstream the dam seawards. This novel subsurface adjustable dam enables flexible desalination of coastal aquifers during the wet periods and effective prevention of active SWI during the dry periods on an annual basis.

## 2 Methods

SEAWAT has been widely used to simulate the seawater intrusion process (Guo and Langevin, 2002). A three-dimensional hypothetical model domain (Figure 2) was used to represent the coastal unconfined aquifer (1000 m × 1000 m × 10 m). The aquifer was assumed to be horizontal, homogeneous, and isotropic. The field-scale model domain was discretized into 10 m × 10 m × 1 m elements. Dirichlet boundary conditions were applied to both the inland and seawater boundaries, with constant heads of 8 m and 9 m, to create the condition of active seawater intrusion. Constant concentrations of 35 g/L and 0 g/L were assigned to the sea and inland boundaries, respectively. The top boundary was defined as a Neumann boundary, with the precipitation recharge. No-flow boundary conditions were applied to all other boundaries. Constant monthly precipitation was used each year (Figure 3), and precipitation recharge into the aquifer was calculated using an infiltration coefficient of 0.33. The wet period was defined as July and August, when precipitation was significantly higher, while the dry period was defined as September to next June. For simplicity, evaporation was neglected.

The aquifer properties and solute transport parameters were adopted from previous seawater intrusion studies (e.g., Lu and Luo, 2010; Chang et al., 2022). The aquifer hydraulic conductivity ($K_f$) was set to 6E-4 m/s, the effective porosity ($\theta$) was 0.3, and the molecular diffusion coefficient was 1E-9 $m^2$/s. The longitudinal dispersivity ($\alpha_L$) was set to 5 m, and the transverse dispersivity ($\alpha_T$) was 1/10 of $\alpha_L$ (Shoemaker, 2004). The dispersivity satisfied the Péclet number requirement ($Pe \approx \frac{\Delta L}{a_L} < 4$) to ensure numerical stability (Voss and Souza, 1987). The structure of the subsurface adjustable dam is illustrated in Figure 2. The adjustable dam, composed of underground dam bodies and sluice gates, is positioned 100 m from the sea boundary. The adjustable dam has a thickness of 1 m, a height equal to the sea level (9 m), and a hydraulic conductivity of 1E-9 m/s. The sluice gates have a length of 10 m, and six gates are evenly spaced within the dam bodies. The sluice gates are opened during the wet period (July and August) and closed during the dry period (September- next June) (Figure 3). All symbols used in the study are summarized in Table 1.

A set of field-scale scenarios were utilized to compare the effects of the SWI (no-barrier), cutoff wall (9 m depth), and subsurface dam (8 m and 9 m height), adjustable subsurface dam (9 m height) scenarios. The length, thickness, position, and hydraulic conductivity of the cutoff wall and subsurface dams were identical to those of the adjustable dam. The simulation period was four years and eight months, with a time step of one day. The simulation period was divided into two phases. In the first phase, seawater intrusion was allowed to occur for 18 months without any physical barriers. The simulated hydraulic head and salinity distribution at the end of the first phase (18th month) were then used as the initial conditions for the second phase. In the second phase, the physical barriers were assumed to be instantaneously installed, and the simulation continued for an additional 38 months.

The toe length of the saltwater wedge (*TL*) and the salt mass in the entire aquifer (*M*) were usually used as evaluation indices of seawater intrusion (Lu et al., 2009; Chang et al., 2023). The *TL* was defined as the distance between the 10% isohaline and the seawater boundary along the aquifer base, and it served as a measure of the extent of seawater intrusion. The *M*, on the other hand, was used to quantify the salinization extent of coastal aquifers.

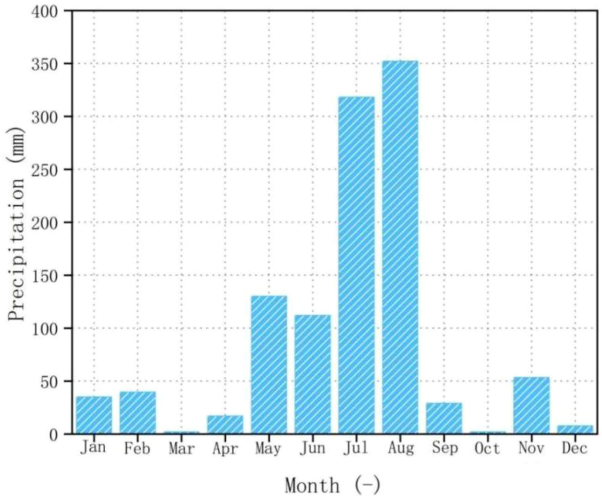


FIGURE 3
Monthly precipitation each year in the numerical simulation.

# 3 Results and discussion

## 3.1 Control effects of traditional subsurface physical barriers

Figure 4 presents the three-dimensional salinity distribution in the SWI and traditional subsurface physical barriers scenarios, and Figure 5 shows the corresponding cross-sectional views of the dynamic salinity distribution. In Figure 4, the semi-transparent gray region represents freshwater, while the non-transparent region represents saltwater, with its color transitioning from red to blue. The blue non-transparent surface corresponds to the 10% seawater salinity contour. Figure 6 records the dynamic variation in the toe length of the saltwater wedge (*TL*) in different scenarios. As shown in Figure 4A, the seawater has intruded inland in the first phase, and the *TL* at 18 months is 158.6 m. These simulated hydraulic head and salinity distributions are then used as the initial conditions for all subsequent simulations in the second phase. In the SWI scenario, the saltwater wedge toe temporarily retreats during July and August due to increased precipitation recharge (Figure 5A), resulting in a decrease in *TL* to 144.5 m at the end of the 2nd August (20th month). Subsequently, *TL* in the SWI scenario gradually increases to 317.2 m at the end of the 5th August (56th month). The dynamic variation of *TL* in the SWI scenario serves as a benchmark for evaluating the control effects of various subsurface physical barriers.

TABLE 1 List of symbols.

| | |
|---|---|
| $c_f$ | freshwater concentration [$ML^{-3}$] |
| $c_s$ | saltwater concentration [$ML^{-3}$] |
| $D$ | molecular diffusion coefficient [$L^2T^{-1}$] |
| $h_f$ | freshwater level [L] |
| $h_s$ | seawater level [L] |
| $K_f$ | hydraulic conductivity [$LT^{-1}$] |
| $M$ | salt mass in the entire aquifer [M] |
| $TL$ | toe length of the saltwater wedge [L] |
| $\alpha_L$ | longitudinal dispersivity [L] |
| $\alpha_T$ | transverse dispersivity [L] |
| $\rho_f$ | freshwater density [$ML^{-3}$] |
| $\rho_s$ | seawater density [$ML^{-3}$] |

The subsurface physical barriers were assumed to be instantaneously constructed 100 m from the sea boundary at the 18th month. Following the installation of the three traditional subsurface physical barriers, the front of the saltwater wedge was trapped upstream the physical barriers, which was known as the residual saltwater (Zheng et al., 2021). Figures 5B-D show that the saltwater continues to intrude inland, indicating that the traditional physical barriers are ineffective in preventing active seawater intrusion. In the 9 m-depth cutoff wall scenario, the toe length of the saltwater wedge (*TL*) briefly decreases below 100 km (at the barrier location) in the 21st and 22nd months (Figure 6), indicating a temporary clean-up of the residual saltwater upstream the wall. However, *TL* resumes its gradual increase after the 22nd month, except for temporary and slight retreats during the wet periods (July and August each year). In the 8 m-height subsurface dam scenario, *TL* retreats gradually to 124 m from the 19th to 21st months, followed by a growth during the next dry period and an again retreat during the subsequent wet period (Figure 6). The difference in *TL* between the 9 m-depth cutoff wall and 8 m-height subsurface dam scenarios decreases year by year, eventually becoming negligible at the 56th month. At the 56th month, *TL* is 257.4 m (9 m-depth cutoff wall) and 240.7 m (8 m-height subsurface dam), respectively. This suggests that the 8 m-height subsurface dam and 9 m-depth cutoff wall are equally ineffective against active SWI. The 9 m-height subsurface dam, which extends to the same height as the sea level, demonstrates a significantly improved ability to mitigate active SWI compared to the cutoff wall and lower subsurface dam (Figure 4). *TL* decreases from 158.6 m to 134.8 m (19th-22nd month) and then mildly

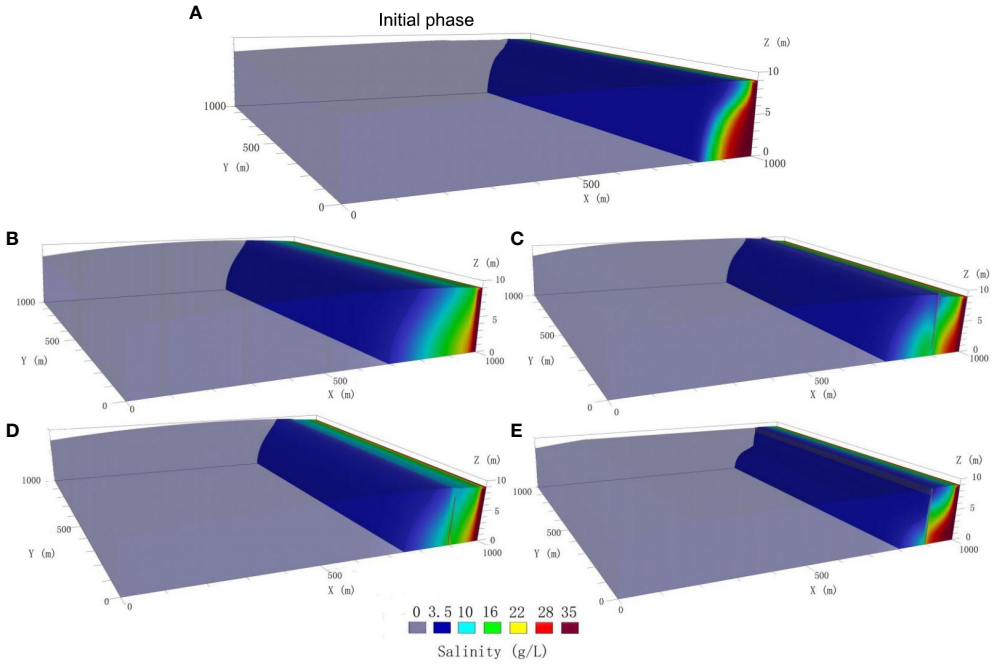


FIGURE 4
Three-dimensional salinity distribution **(A)** at 18th month (June, 2nd year, dry period) and at 56th month (August, 5th year, wet period) in the scenarios of **(B)** SWI, **(C)** cutoff wall (9 m-depth), **(D)** subsurface dam (8 m-height), **(E)** subsurface dam (9 m-height). The gray blocks represent the subsurface physical barriers.

increases monotonically over time. At the 56th month, *TL* is 195.2 m (9 m-height subsurface dam), which is considerably shorter than that of the other scenarios in Figure 6. This indicates that even a subsurface dam as high as the sea level is insufficient to prevent active SWI, although it substantially reduces the rate of seawater intrusion (Figure 5D). In conclusion, the traditional subsurface physical barriers can mitigate the velocity of active seawater intrusion, but they are ultimately unable to prevent it.

## 3.2 Control effects of the subsurface adjustable dam

The subsurface adjustable dam (9 m height) was also assumed to be installed instantaneously at 18th month, 100 m from the sea boundary. The sluice gates were configured to be open during the wet periods (July and August) and closed during the dry periods (September-next June). Figure 7 presents cross-sectional views of the dynamic salinity distribution in the adjustable dam scenario. The toe length of the saltwater wedge (*TL*) varies at different locations along the adjustable dam. The longest *TL* is observed at the middle of the dam body (Figure 7A), while the shortest *TL* is located at the middle of the sluice gate (Figure 7B). Figure 8 illustrates the three-dimensional salinity distribution in the subsurface adjustable dam scenario at the 54th and 56th months. When precipitation recharge is minimal during the dry period, the sluice gates are closed, effectively blocking the path of active seawater intrusion and confining the residual saltwater upstream the dam (Figure 8A). Conversely, during the wet period when precipitation increases significantly, the sluice gates are opened to discharge inland groundwater (Figure 8B). The upstream residual saltwater is also transported seawards through the sluice gate openings. As shown in Figure 7B, the upstream residual saltwater at the middle of the sluice gates is gradually removed over time, meanwhile the upstream residual saltwater at the middle of the dam bodies is also significantly reduced (Figure 7A).

Figure 9 illustrates the dynamic variation in the toe length of the saltwater wedge (*TL*) in the subsurface adjustable dam scenario at the middle of the dam body and the sluice gate. As shown in Figure 9, the *TL* at both the dam body and the sluice gate increases during the dry periods (September-next June). During the wet periods (July and August), the opening of the sluice gates accelerates groundwater discharge, enhancing the desalination process near the sluice gates and causing a more pronounced retreat of the saltwater wedge. Notably, the *TL* at the middle of the sluice gate declines more significantly than that at the middle of the dam body during each wet period. Furthermore, the *TL* at the middle of the sluice gate decreases to 86.7 m at the 31st month, indicating that the upstream residual saltwater has been completely removed. Subsequently, the saltwater wedge toe at the sluice gate never exceeds the dam location again. In contrast, the upstream residual saltwater at the middle of the dam body is cleared more gradually (Figure 7A). The fluctuation range of the *TL* at the middle of the dam body is less pronounced than that at the sluice gate (Figure 9), and the *TL* at the middle of the dam body never exceeds its initial value. Thus, the saltwater wedge at any location has receded each year since the installation of the adjustable dam, demonstrating the effectiveness of the dam in preventing active seawater intrusion.

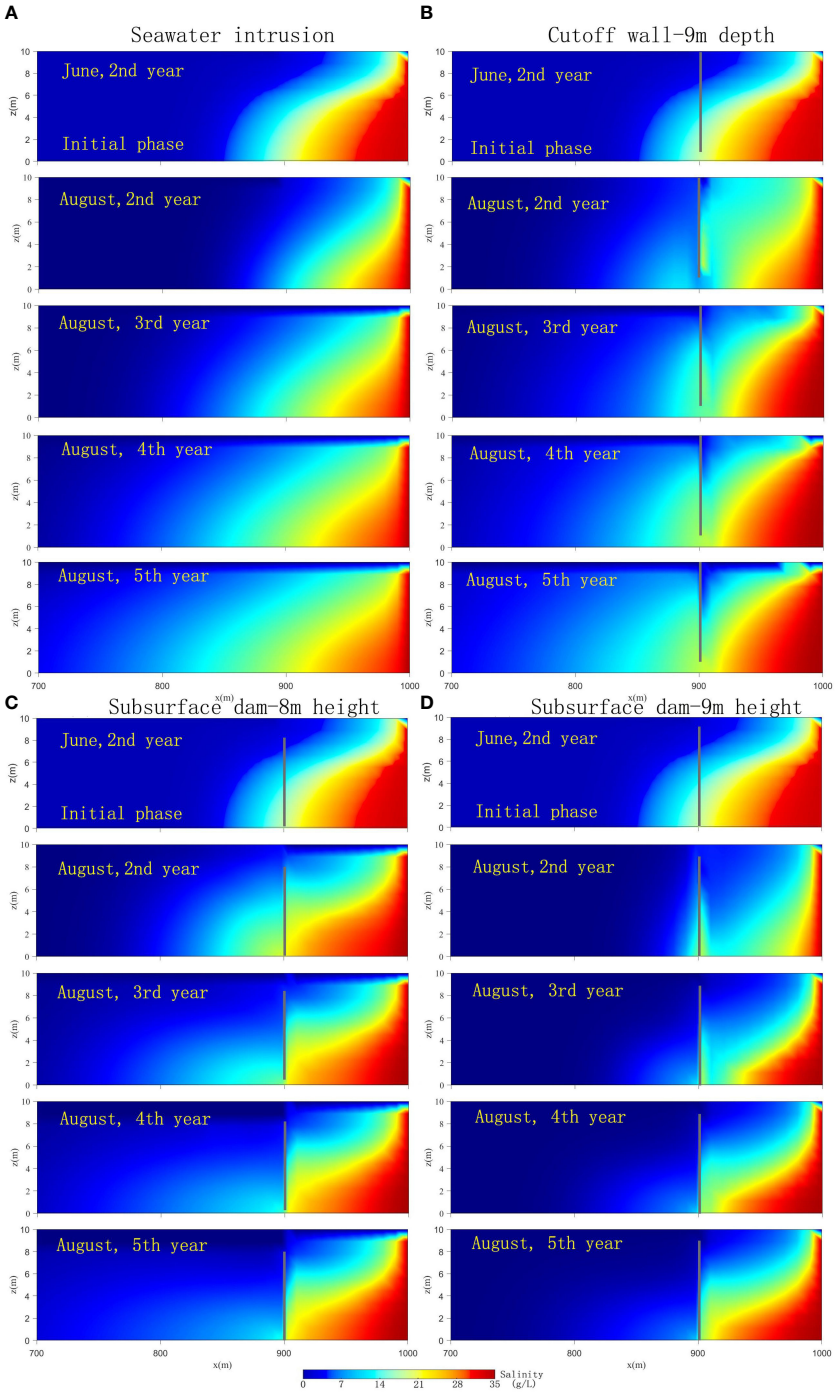


FIGURE 5
Cross-section of the dynamic salinity distribution in the **(A)** SWI, **(B)** cutoff wall (9 m-depth), **(C)** subsurface dam (8 m-height), and **(D)** subsurface dam (9 m-height) scenarios on an annual basis.

## 3.3 Groundwater desalination in different physical barriers scenarios

Figure 10 presents the salt mass in the entire aquifer (*M*) for all SWI and physical barriers scenarios. Notably, *M* peaks before the beginning of July each year in all scenarios. This is because the saltwater wedge keeps intruding during the dry periods (September-next June). However, *M* decreases during July and August due to the increased precipitation recharge, then reaching its lowest value at the end of August. Subsequently, as the precipitation recharge decreases again, seawater intrusion resumes, leading to an increase in *M*.

Compared to the SWI scenario, all the subsurface physical barriers could reduce the salt mass (*M*) to varying degrees throughout the simulation period. However, the overall trend of *M* in the SWI, cutoff wall, and subsurface dam scenarios

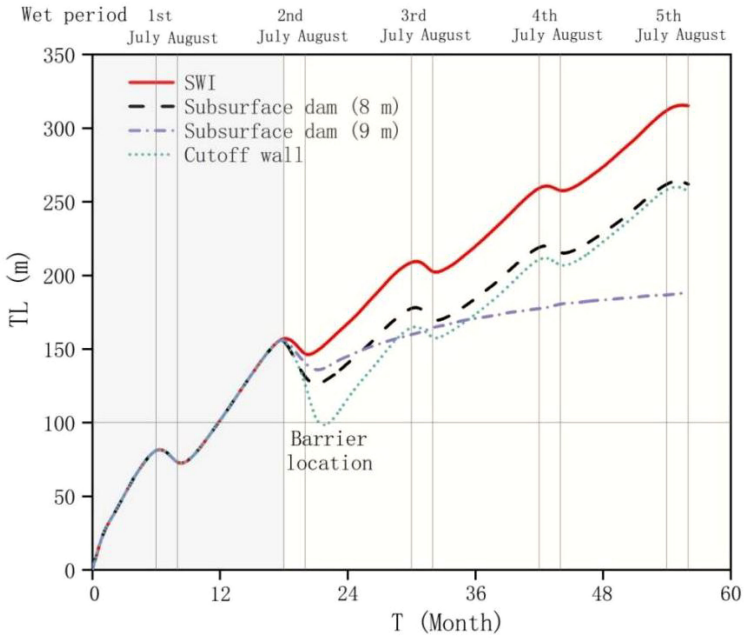


FIGURE 6
Dynamic variation in the toe length of the saltwater wedge in the SWI, subsurface dams (8 m-height and 9 m-height), and cutoff wall (9 m-depth) scenarios. The gray region represents the period without subsurface barriers, and the light yellow region means the period after the construction of subsurface barriers.

increase each year, despite temporary decrease during the wet periods (July and August). The *M* values in the 9 m-depth cutoff wall and 8 m-height subsurface dam scenarios are similar and slightly lower than that in the SWI case. In contrast, *M* in the 9 m-height subsurface dam scenario increases mildly and is significantly lower than that in the SWI case. These results indicate that the traditional physical barriers temporarily reduce the saltwater during the wet periods, but this reduction is offset by increased seawater intrusion during the next dry periods. Conversely, the overall trend of *M* in the subsurface adjustable dam scenario gradually decreases each year. This is because the residual saltwater upstream the adjustable dam is gradually removed when the sluice gates are open during the wet periods, meanwhile the downstream saltwater is prevented from intruding inland during the dry periods by the closed sluice gates.

In summary, the traditional subsurface physical barriers (cutoff wall and subsurface dam) are ineffective in preventing active seawater intrusion and desalinating the residual saltwater. In contrast, the subsurface adjustable dam can not only prevent the seawater from intruding inland during the dry periods but also remove the residual saltwater trapped upstream the dam during the wet periods.

## 4 Discussion

In contrast to conventional subsurface physical barriers, researchers have explored novel techniques to prevent SWI, such as mixed physical barrier (Abdoulhalik and Ahmed, 2017), variable permeability full-section wall (Zheng et al., 2020), and geochemical cutoff wall (Laabidi and Bouhlila, 2021). However, these structures remained fixed and lacked the ability to prevent active SWI. Our proposed adjustable dam adopts a proactive approach to coastal groundwater management. Operators can dynamically control the opening and closing of sluice gates based on real-time precipitation data. This enables the storage of groundwater resources and the prevention of active SWI during the dry periods. Conversely, during the wet periods, operators can open the sluice gates to discharge upstream groundwater and remove the residual saltwater, thereby improving water quality. Thus, this innovative approach simultaneously addresses the challenges of active SWI and the residual saltwater upstream of dams in coastal aquifers.

The dam bodies of subsurface adjustable dam can be constructed via excavation or grouting, utilizing low-permeability materials such as clay or cement mortar (Molfetta and Sethi, 2006; Yang et al., 2022). The height of the dam bodies must exceed the sea level to effectively intercept active SWI. In our numerical simulations, we assumed a constant sea level for simplicity. However, in practical applications, the adjustable dam should be designed to withstand the highest local tide level. Trenches are excavated in advance, and the soil on both sides is supported by porous grids. The sluice gates are positioned between these porous grates. The design of the sluice gates can vary depending on hydrogeological conditions and may include steel, cement, or rubber materials. The gates can be raised or

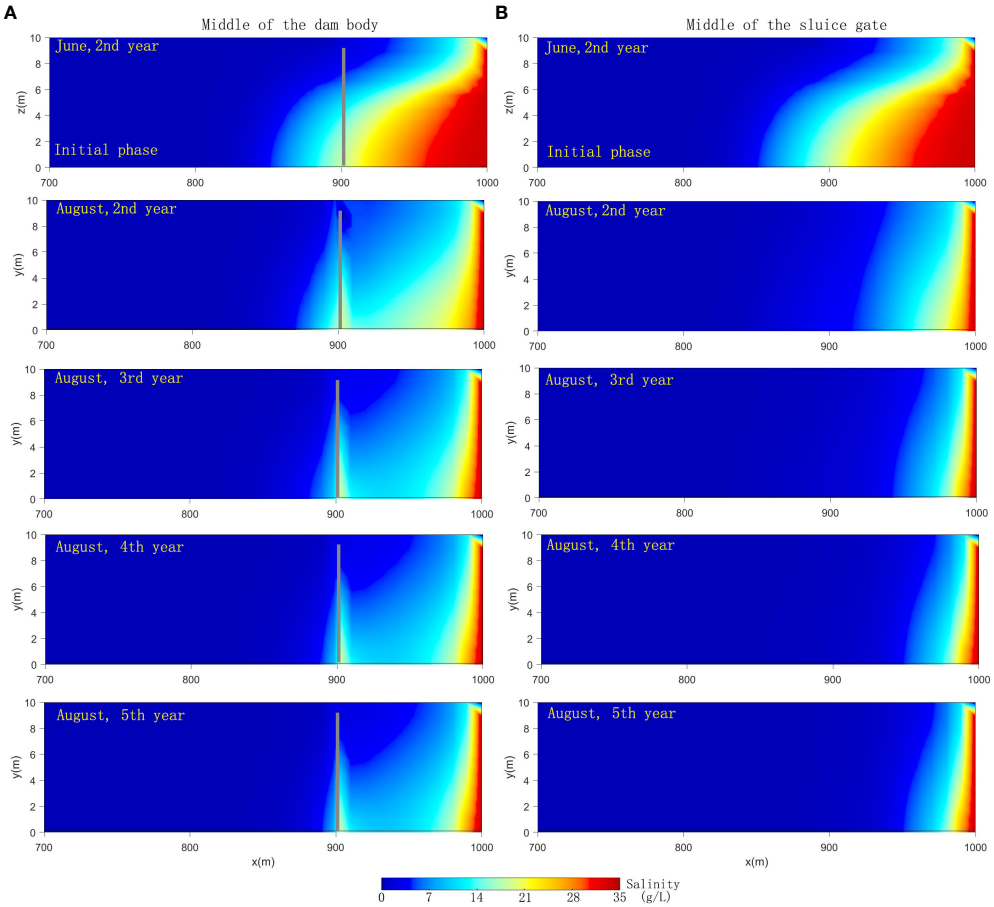


FIGURE 7
Cross-section of the salinity distribution at the **(A)** the middle of the dam body and **(B)** the middle of the sluice gate in the adjustable dam scenario on an annual basis.

lowered using a crane. Meanwhile the sluice gates can also be made into tank shapes which can lowered or raised by injecting or pumping water. Real-time monitoring of groundwater levels via monitoring wells allows for dynamic adjustment of the sluice gates based on precipitation and groundwater level variations. This enables flexible management of coastal groundwater resources, akin to the operation of surface reservoirs.

## 5 Summary and conclusion

The traditional subsurface physical barriers for preventing SWI, such as cutoff walls and subsurface dams, have fixed structures and cannot adapt to dynamic variations in precipitation. To address this limitation, we have designed a novel subsurface adjustable dam consisting of sluice gates and dam bodies. This innovative structure aims to prevent active seawater intrusion and desalinate the residual saltwater upstream the dam. To evaluate the effectiveness of the novel subsurface adjustable dam, we conducted a series of field-scale numerical simulations and compared its performance to those of traditional subsurface physical barriers. The key findings are summarized below.

1. Compared to the scenario without any subsurface physical barriers, all the subsurface physical barriers reduced the toe length of the saltwater wedge (*TL*) and the total salt mass within the aquifer (*M*) in varying degrees under the condition of active seawater intrusion. Among the traditional subsurface physical barriers, the 9 m-depth cutoff wall and the 8 m-height subsurface dam exhibited comparable control effects, although they were less effective than the 9 m-height subsurface dam (as high as the sea level). Notably, the novel subsurface adjustable dam demonstrated superior control on active seawater intrusion compared to all other traditional barrier types.
2. The traditional subsurface physical barriers could slow down active seawater intrusion process each year, while they failed in blocking active seawater intrusion completely. Meanwhile, although the traditional physical barriers could temporarily reduce the upstream residual saltwater in the wet period, the salt mass will increased more in the next dry period. Consequently, the overall salt mass in the cutoff wall and subsurface dam scenarios gradually increased on an annual basis, indicating that these traditional barriers lacked the capacity to desalinate the upstream residual saltwater.

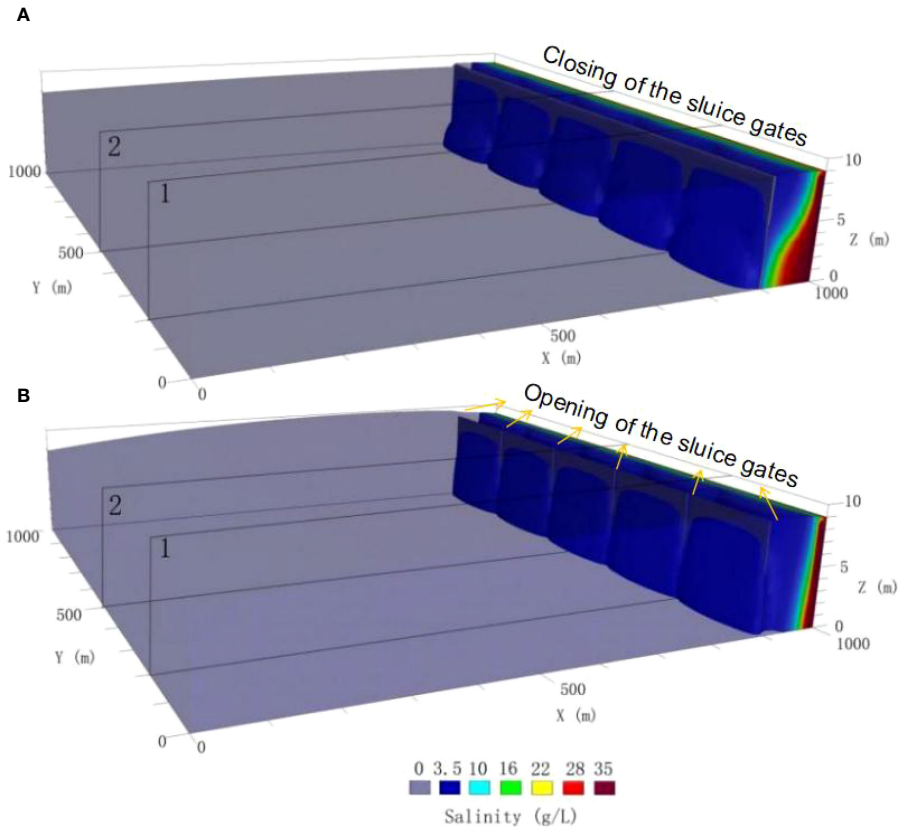


FIGURE 8
Three-dimensional salinity distribution in the adjustable dam scenario at the **(A)** 54th month (June, 5th year, dry period) and **(B)** 56th month (August, 5th year, wet period). The gray block represents the adjustable dam. The cross section 1 locates the middle of the sluice gate, and the cross section 2 locates the middle of the dam body.

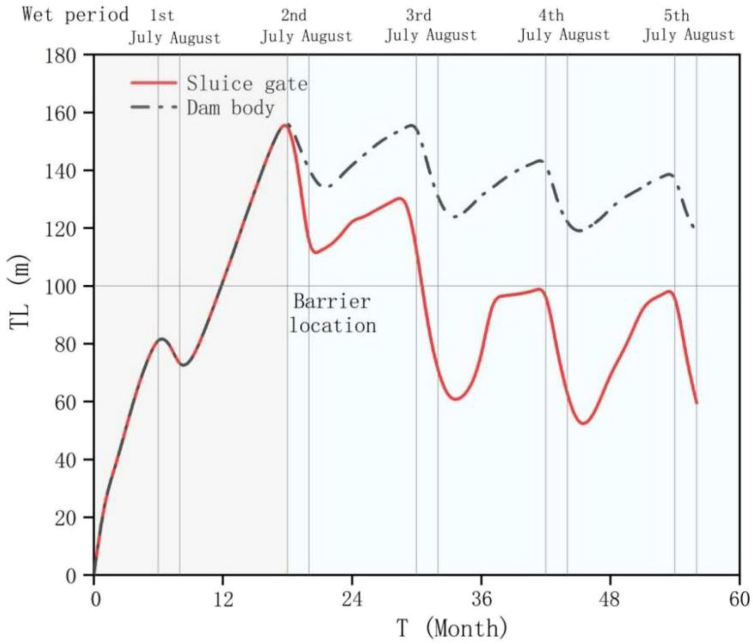


FIGURE 9
Dynamic variation in the toe length of the saltwater wedge in the subsurface adjustable dam scenario. The gray region represents the period without subsurface barriers, and the light blue region means the period after the construction of the adjustable dam.

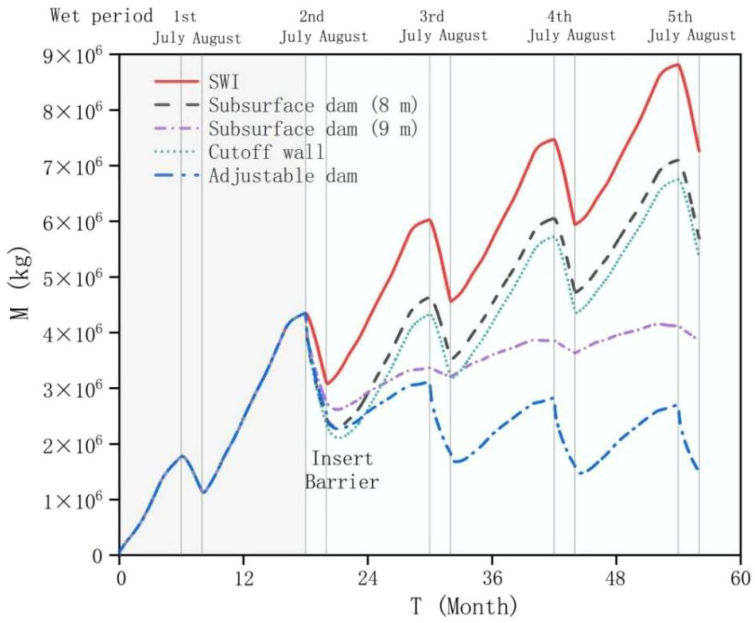


FIGURE 10
Dynamic variation of salt mass in the entire aquifer over time in different physical barriers scenarios. The gray region represents the period without subsurface barriers, and the light blue region means the period after the construction of subsurface barriers.

3. The novel subsurface adjustable dam could be dynamically regulated in response to the seasonal variation in precipitation. When the precipitation recharge was small during the dry period, the sluice gates were closed, then the path of active seawater intrusion was obstructed completely. During the wet period, the sluice gates were opened due to the large precipitation, the upstream residual saltwater was gradually removed through the opened sluice gates. Thus, both the toe length of saltwater wedge and the salt mass in the entire aquifer decreased each year attributing to the flexible adjustment ability of the novel dam. The above conclusion indicated that the subsurface adjustable dam was an effective measure which prevented active seawater intrusion and eliminated the upstream residual saltwater at the same time.

In this study, we have designed a novel adjustable dam and demonstrated its effectiveness in preventing active seawater intrusion and desalinating the upstream residual saltwater in coastal aquifers. Building on our prior studies (Chang et al., 2019, 2023), we have identified the hydraulic gradient as a pivotal determinant in the efficacy of physical barriers against seawater intrusion. The most unfavorable hydraulic gradient conditions are caused by the highest local tidal level and the lowest rainfall recharge. In the realm of field engineering, the design of physical barriers against seawater intrusion typically incorporates the highest recorded local tide level as a reference sea level. Thus, in this study, we assumed a constant sea level and seasonal variations in rainfall to simplify the numerical model.

## Data availability statement

The original contributions presented in the study are included in the article/supplementary material. Further inquiries can be directed to the corresponding author.

## Author contributions

QC: Conceptualization, Data curation, Formal analysis, Funding acquisition, Investigation, Methodology, Project administration, Resources, Software, Supervision, Validation, Visualization, Writing – original draft, Writing – review & editing. CG: Data curation, Investigation, Methodology, Validation, Visualization, Writing – original draft, Writing – review & editing. XZ: Conceptualization, Data curation, Formal analysis, Funding acquisition, Investigation, Methodology, Project administration, Resources, Software, Supervision, Validation, Visualization, Writing – original draft, Writing – review & editing. YL: Formal analysis, Investigation, Methodology, Visualization, Writing – original draft. XS: Methodology, Resources, Visualization, Writing – original draft.

## Funding

The author(s) declare financial support was received for the research, authorship, and/or publication of this article. This work was supported by the National Natural Science Foundation of

China (No.42307069) and (No.42272282), the Shandong Provincial Natural Science Foundation (ZR2023QD019), the China Postdoctoral Science Foundation (2023T160609), the Postdoctoral Innovation Project of Shandong Province (SDCX-ZG-202203080), the Ecological Restoration Project of Qingdao (20220294), and the Fundamental Research Funds for the Central Universities (202461074).

## Acknowledgments

We thank the editor and reviewers whose critical and constructive comments have helped us improve the quality of the manuscript greatly.

## Conflict of interest

The authors declare that the research was conducted in the absence of any commercial or financial relationships that could be construed as a potential conflict of interest.

## Publisher's note

All claims expressed in this article are solely those of the authors and do not necessarily represent those of their affiliated organizations, or those of the publisher, the editors and the reviewers. Any product that may be evaluated in this article, or claim that may be made by its manufacturer, is not guaranteed or endorsed by the publisher.

## References

Abdoulhalik, A., and Ahmed, A. A. (2017). The effectiveness of cutoff walls to control saltwater intrusion in multi-layered coastal aquifers: Experimental and numerical study. *J. Environ. Manage.* 199, 62–73. doi: 10.1016/j.jenvman.2017.05.040

Badaruddin, S., Werner, A. D., and Morgan, L. K. (2017). Characteristics of active seawater intrusion. *J. Hydrol.* 551, 632–647. doi: 10.1016/j.jhydrol.2017.04.031

Blowes, D. W., Ptacek, C. J., Benner, S. G., McRae, C. W. T., Bennett, T. A., and Puls, R. W. (2000). Treatment of inorganic contaminants using permeable reactive barriers. *J. Contam. Hydrol.* 45, 123–137. doi: 10.1016/S0169-7722(00)00122-4

Chang, Q., Zheng, T., Chen, Y., Zheng, X., and Walther, M. (2020). Investigation of the elevation of saltwater wedge due to subsurface dams. *Hydrol. Processes* 32, 4251–4261. doi: 10.1002/hyp.13863

Chang, Q., Zheng, T., Chen, Y., Zheng, X., and Walther, M. (2021). Influence of inland freshwater influx on the natural desalination of coastal aquifers with a cutoff wall. *Desalination* 499, 114863. doi: 10.1016/j.desal.2020.114863

Chang, Q., Zheng, T., Gao, C., Zheng, X., Lin, Y., Song, X., et al. (2024). Hydrodynamic behavior of freshwater-saltwater mixing zone in the context of subsurface physical barriers. *J. Environ. Manage.* 353, 120080. doi: 10.1016/j.jenvman.2024.120080

Chang, Q., Zheng, T., Gao, C., Zheng, X., and Walther, M. (2022). How to cope with downstream groundwater deterioration induced by cutoff walls in coastal aquifers. *J. Hydrol.* 610, 127804. doi: 10.1016/j.jhydrol.2022.127804

Chang, Q., Zheng, T., Zheng, X., Gao, C., Song, X., and Walther, M. (2023). Repulsion driven by groundwater level difference around cutoff walls on seawater intrusion in unconfined aquifers. *Sci. Total Environ.* 874, 162535. doi: 10.1016/j.scitotenv.2023.162535

Chang, Q., Zheng, T., Zheng, X., Zhang, B., Sun, Q., and Walther, M. (2019). Effect of subsurface dams on saltwater intrusion and fresh groundwater discharge. *J. Hydrol.* 576, 508–519. doi: 10.1016/j.jhydrol.2019.06.060

Fang, Y., Zheng, T., Wang, H., Guan, R., Zheng, X., and Walther, M. (2021). Experimental and numerical evidence on the influence of tidal activity on the effectiveness of subsurface dams. *J. Hydrol.*, 127149. doi: 10.1016/j.jhydrol.2021.127149

Gao, M., Zheng, T., Chang, Q., Zheng, X., and Walther, M. (2021). Effects of mixed physical barrier on residual saltwater removal and groundwater discharge in coastal aquifers. *Hydrol. Processes* 35, e14263. doi: 10.1002/hyp.14263

Gao, S., Zheng, T., Zheng, X., and Walther, M. (2022). Influence of layered heterogeneity on nitrate enrichment induced by cut-off walls in coastal aquifers. *J. Hydrol.* 609, 127722. doi: 10.1016/j.jhydrol.2022.127722

Guo, W., and Langevin, C. D. (2002). *User's Guide to SEAWAT: A Computer Program for Simulation of Three-Dimensional Variable-Density Groundwater Flow* (Tallahassee, Florida: US Geological Survey Techniques of Water Resources Investigations 6-A7). doi: 10.3133/ofr01434

Ishida, S., Tsuchihara, T., Yoshimoto, S., and Imaizumi, M. (2011). Sustainable use of groundwater with underground dams. *Japan Agric. Res. Q.* 45, 51–61. doi: 10.6090/jarq.45.51

Kaleris, V. K., and Ziogas, A. I. (2013). The effect of cutoff walls on saltwater intrusion and groundwater extraction in coastal aquifers. *J. Hydrol.* 476, 370–383. doi: 10.1016/j.jhydrol.2012.11.007

Kang, P., and Xu, S. (2017). The impact of an underground cut-off wall on nutrient dynamics in groundwater in the lower Wang River watershed, China. *Isotopes Environ. Health Stud.* 53, 36–53. doi: 10.1080/10256016.2016.1186670

Kong, J., Gao, C., Jiang, C., Wang, J., Gao, X., and Jing, L. (2023). Effect of the cutoff wall on the fate of nitrate in coastal unconfined aquifers under tidal action. *Front. Mar. Sci.* 10. doi: 10.3389/fmars.2023.1135072

Laabidi, E., and Bouhlila, R. (2021). A new technique of seawater intrusion control: development of geochemical cutoff wall. *Environ. Sci. Pollut. Res.* 28, 41794–41806. doi: 10.1007/s11356-021-13677-0

LeRoux, N. K., Frey, S. K., Lapen, D. R., Guimond, J. A., and Kurylyk, B. L. (2023). Mega-tidal and surface flooding controls on coastal groundwater and saltwater intrusion within agricultural dikelands. *Water Resour. Res.* 59, 1–21. doi: 10.1029/2023WR035054

Lu, C., Chen, Y., Zhang, C., and Luo, J. (2013). Steady-state freshwater-seawater mixing zone in stratified coastal aquifers. *J. Hydrol.* 505, 24–34. doi: 10.1016/j.jhydrol.2013.09.017

Lu, C., Kitanidis, P. K., and Luo, J. (2009). Effects of kinetic mass transfer and transient flow conditions on widening mixing zones in coastal aquifers. *Water Resour. Res.* 45, 1–17. doi: 10.1029/2008WR007643

Lu, C., and Luo, J. (2010). Dynamics of freshwater-seawater mixing zone development in dual-domain formations. *Water Resour. Res.* 46, 1–6. doi: 10.1029/2010WR009344

Luyun, R., Momii, K., and Nakagawa, K. (2011). Effects of recharge wells and flow barriers on seawater intrusion. *Ground Water* 49, 239–249. doi: 10.1111/gwat.2011.49.issue-2

Molfetta, A. D., and Sethi, R. (2006). Clamshell excavation of a permeable reactive barrier. *Environmental Geology.* 50, 361–369. doi: 10.1007/s00254-006-0215-3

Orton, P., Ralston, D., van Prooijen, B., Secor, D., Ganju, N., Chen, Z., et al. (2023). Increased utilization of storm surge barriers: A research agenda on estuary impacts. *Earth's Future* 11, e2022EF002991. doi: 10.1029/2022EF002991

Shen, Y., Xin, P., and Yu, X. (2020). Combined effect of cutoff wall and tides on groundwater flow and salinity distribution in coastal unconfined aquifers. *J. Hydrol.* 581, 124444. doi: 10.1016/j.jhydrol.2019.124444

Shoemaker, W. B. (2004). Important observations and parameters for a salt water intrusion model. *Ground Water* 42, 829–840. doi: 10.1111/j.1745-6584.2004.t01-2-.x

Sun, Q., Zheng, T., Zheng, X., Chang, Q., and Walther, M. (2019). Influence of a subsurface dam on nitrate contamination in an unconfined aquifer. *J. Hydrol.* 575, 234–243. doi: 10.1016/j.jhydrol.2019.05.030

Voss, C. I., and Souza, W. R. (1987). Variable density flow and solute transport simulation of regional aquifers containing a narrow freshwater-saltwater mixing zone. *Water Resour. Res.* 23, 1851–1866. doi: 10.1029/WR023i010p01851

Wang, J., Kong, J., Gao, C., and Zhou, L. (2023). Effect of mixed physical barrier on seawater intrusion and nitrate accumulation in coastal unconfined aquifers. *Environ. Sci. Pollut. Res.* 30, 105308–105328. doi: 10.1007/s11356-023-29637-9

Yang, Y. L., Reddy, K. R., Zhang, T., Fan, R. D., Fu, X. L., and Du, Y. J. (2022). Enhanced contaminant retardation by novel modified calcium bentonite backfill in slurry trench cutoff walls. *Construct. Build. Mater.* 320, 126285. doi: 10.1016/j.conbuildmat.2021.126285

Yin, J., Wang, N., Lu, C., Tsai, F. T. C., and Chen, H. (2023). Fast desalinization of residual saltwater using subsurface dams combined with saltwater discharge or freshwater recharge. *J. Hydrol.* 619, 129282. doi: 10.1016/j.jhydrol.2023.129282

Zheng, T., Gao, M., Chang, Q., Zheng, X., and Walther, M. (2022). Dynamic desalination of intruding seawater after construction of cut-off walls in a coastal unconfined aquifer. *Front. Mar. Sci.* 9. doi: 10.3389/fmars.2022.857807

Zheng, T., Zheng, X., Chang, Q., Zhan, H., and Walther, M. (2021). Timescale and effectiveness of residual saltwater desalinization behind subsurface dams in an unconfined aquifer. *Water Resour. Res.* 57, e2020WR028493. doi: 10.1029/2020WR028493

Zheng, T., Zheng, X., Sun, Q., Wang, L., and Walther, M. (2020). Insights of variable permeability full-section wall for enhanced control of seawater intrusion and nitrate contamination in unconfined aquifers. *J. Hydrol.* 586, 124831. doi: 10.1016/j.jhydrol.2020.124831